Science Advances

AAAS

advances.sciencemag.org/cgi/content/full/4/1/eaao6718/DC1

Supplementary Materials for

Stereochemistry and amyloid inhibition: Asymmetric triplex metallohelices enantioselectively bind to Aβ peptide

Yijia Guan, Zhi Du, Nan Gao, Yue Cao, Xiaohui Wang, Peter Scott, Hualong Song, Jinsong Ren, Xiaogang Qu

Published 19 January 2018, *Sci. Adv.* **4**, eaao6718 (2018)
DOI: 10.1126/sciadv.aao6718

This PDF file includes:

- fig. S16. Cyclic voltammograms corresponding to the $O_2/O_2^{\bullet}$ redox couple.
- fig. S17. Effect of the metallohelices on ROS production in PC12 cells.
- fig. S18. Absorption spectra of 5 μM metallohelices in water and PBS.
- fig. S19. Effect of A1 and B4 on PC12 cell viability determined by MTT.
- fig. S20. Protection effects of metallohelices on Aβ40- and Aβ42-induced cytotoxicity of PC12 cells.
- table S1. IC_{50} values of metallohelices A1 and B4 for the inhibition of fibril formation and destabilization of the preformed fibrils.
- table S2. Analysis of fluorescence titration and ITC data.
- table S3. Enthalpy (ΔH), entropy (ΔS), and Gibbs free energy (ΔG) of the binding of Aβ with metallohelices at pH 7.3.

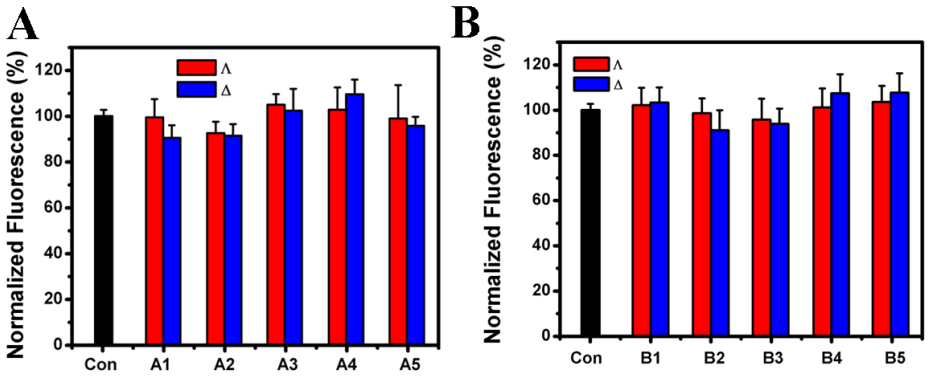

fig. S1. Influence of these metal complexes on the fluorescence of ECFP (a non-Aβ fusion system). Values exhibit mean ± SD and independent experiments were performed three times.

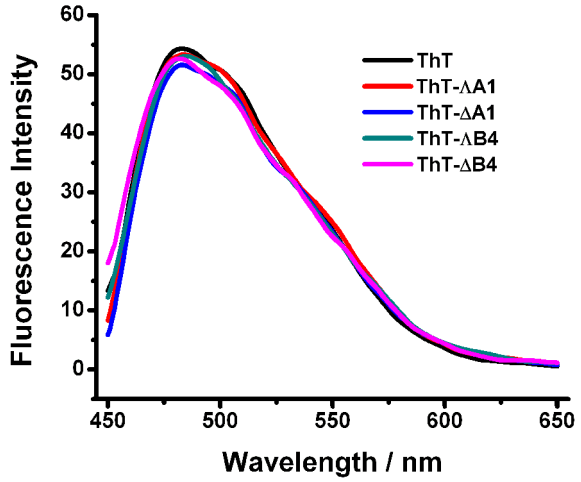

fig. S2. The influence of these metallohelices on the fluorescence of ThT.

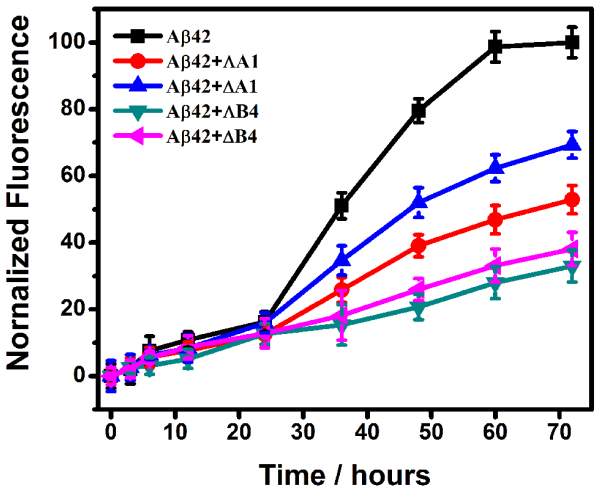

fig. S3. Aggregation kinetics of Aβ42 monitored by ThT assay in the absence or presence of A1 and B4.

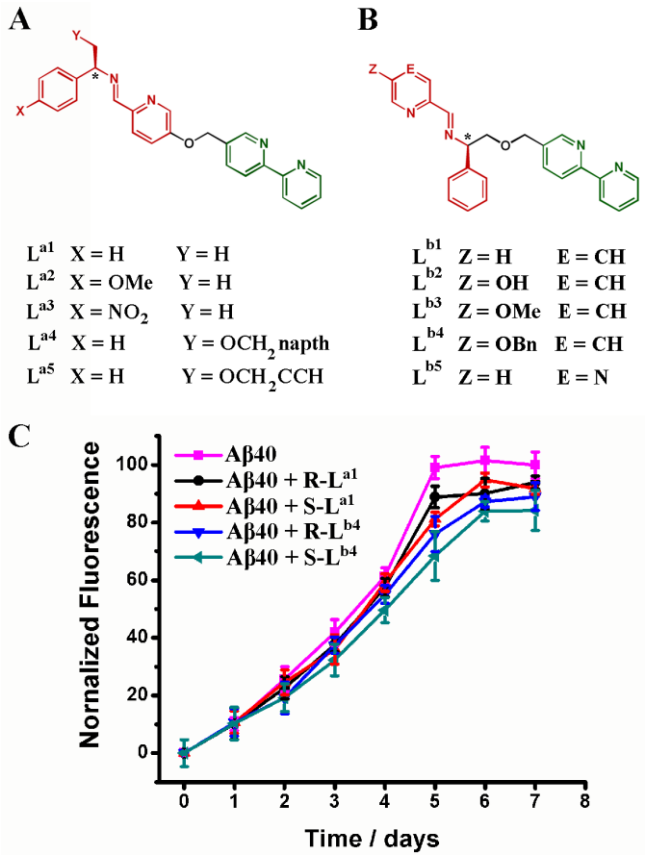

fig. S4. Aggregation kinetics of Aβ40 monitored by ThT assay in the absence or presence of the ligands of A1 and B4. (**A**, **B**) The directional ligands of metallohelice enantiomers. The signal of star represents chiral carbon. (**C**) Fibrillation kinetics of Aβ40 was monitored by the development of thioflavin T binding in the absence or presence of different ligands. [Aβ40] = 50 μM, [ligands] = 10 μM. Values exhibit mean ± SD and independent experiments were performed three times.

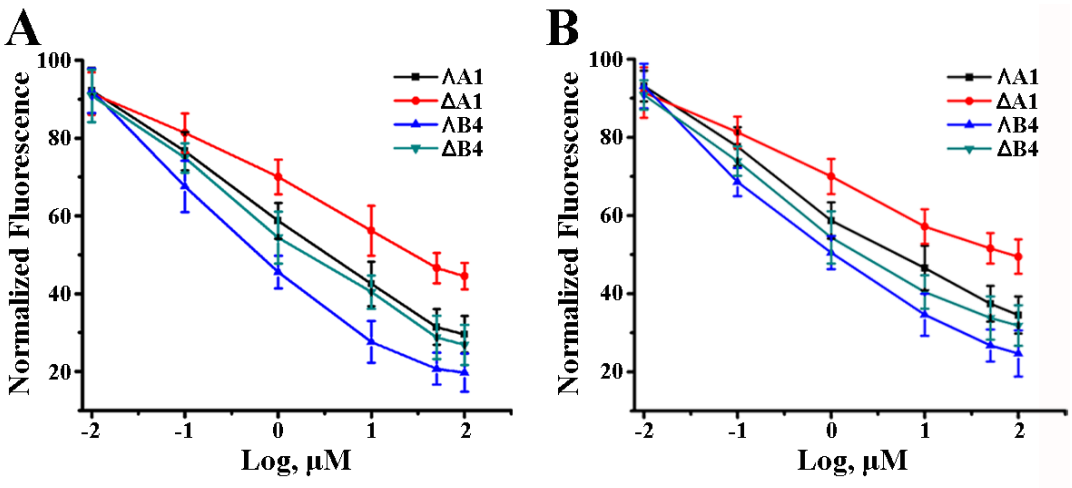

fig. S5. The inhibition effect of A1 and B4 on Aβ40/Aβ42 fibrillogenesis at different concentrations. (**A**) Concentration dependent inhibition of Aβ40 fibrillogenesis by complex A1 and complex B4. (**B**) Concentration dependent inhibition of Aβ42 fibrillogenesis by metallohelices A1 and metallohelices B4. The concentrations of Aβ40 and Aβ42 were 50 μM. Values exhibit mean ± SD and independent experiments were performed three times.

table S1. IC_{50} values of metallohelices A1 and B4 for the inhibition of fibril formation and destabilization of the preformed fibrils.

Metallohelices		IC_{50}	
		Inhibition (μM)	Destabilization (μM)
Asymmetric Metallohelices	ΛA1	3.65±0.53	3.93±0.67
	ΔA1	32.29±3.61	41.6±5.31
	ΛB4	0.94±0.17	1.21±0.74
	ΔB4	2.55±0.36	2.63±0.52
Symmetric Metallohelices	Λ1	1.69±0.23	1.97±0.46
	Δ1	5.43±0.86	8.53±0.71
	Λ2	6.62±0.58	9.82±1.23
	Δ2	42.21±6.13	>50

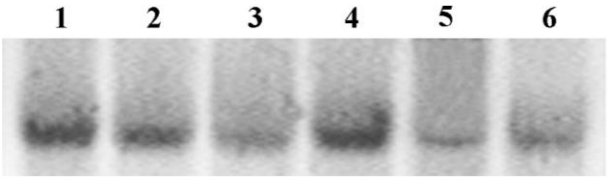

fig. S6. The inhibition effect of the metallohelices on Aβ40 aggregation measured by SDS-PAGE. 1) Control (Aβ40 monomer), **2**) Aβ40 fibrils, **3**) Aβ40-ΛA1, **4**) Aβ40-ΔA1, **5**) Aβ40-ΛB4, **6**) Aβ40-ΔB4. The samples of 2)~6) were incubated at 37 °C for 7 days and separated by centrifugation. The pellets were resuspended and boiled after the addition of sample buffer. Samples were run on a 12% Tris-tricine SDS gel at 120 V for 1 hour, followed by silver staining.

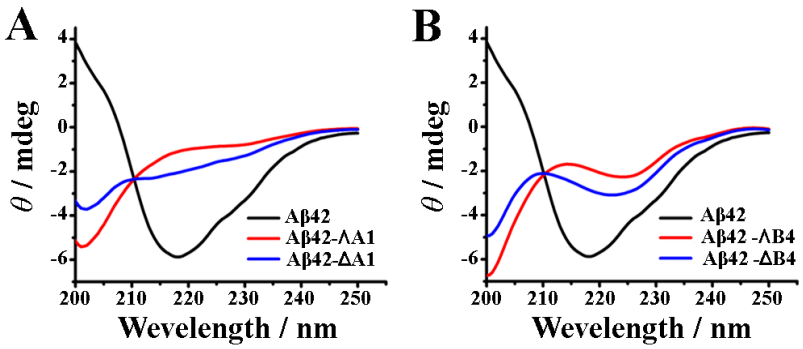

fig. S7. The influence of A1 and B4 on the second structures of Aβ42 monitored by CD. (**A**) CD spectra of Aβ42 with or without the incubation of ΛA1 and ΔA1, (**B**) CD spectra of Aβ42 with or without the incubation of ΛB4 and ΔB4.

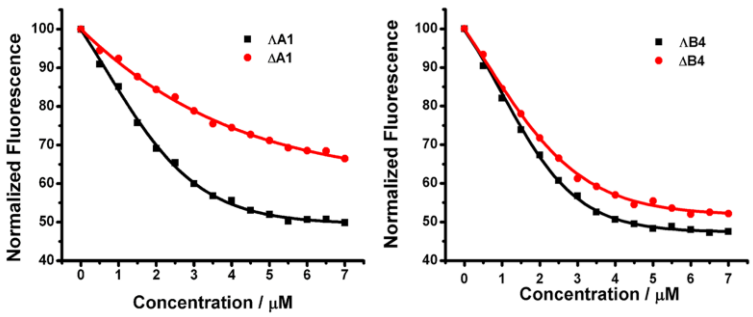

fig. S8. Fluorescence titration of Aβ40 (3 μM) with various concentrations of metallohelices in 20 mM tris buffer. The excitation wavelength was 278 nm and the emission intensity at 306 nm was used for analysis.

table S2. Analysis of fluorescence titration and ITC data.

Metallohelices		Titration		ITC	
		K_a (M^{-1})	ΔG_b (kJ mol^{-1})	K_a (M^{-1})	ΔG_b (kJ mol^{-1})
Asymmetric Metallohelices	ΛA1	(4.19±0.88)×10^6	-37.78±3.52	(4.93±0.48)×10^6	-38.18±3.28
	ΔA1	(4.71±0.92)×10^5	-32.36±2.62	(5.36±1.03)×10^5	-32.68±2.66
	ΛB4	(8.43±1.37)×10^6	-39.51±2.71	(8.41±1.55)×10^6	-39.50±3.76
	ΔB4	(3.64±0.43)×10^6	-37.43±2.24	(3.01±0.29)×10^6	-36.96±2.07
Symmetric Metallohelices	Λ1	(3.81±0.64)×10^6	-37.54±2.40		
	Δ1	(9.62±2.72)×10^5	-34.13±3.05		
	Λ2	(1.04±0.26)×10^6	-34.33±3.03		
	Δ2	(1.97±0.38)×10^5	-30.20±2.26		

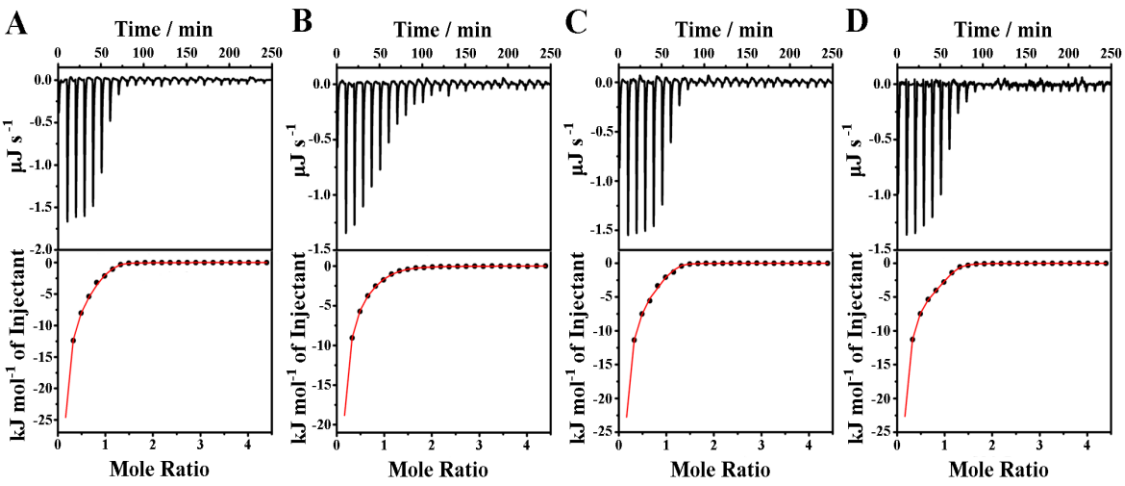

fig. S9. ITC data for the Aβ40 titrations with metallohelices. (**A**) ΛA1, (**B**) ΔA1, (**C**) ΛB4, and (**D**) ΔB.

table S3. Enthalpy (Δ*H*), entropy (Δ*S*), and Gibbs free energy (Δ*G*) of the binding of Aβ with metallohelices at pH 7.3.

Sample	ΔH （KJ/mol）	TΔS （KJ/mol）	ΔG=ΔH-TΔS （KJ/mol）	K_a (M^{-1})
ΛA1	-24.93	13.26	-38.19	(4.93±0.48)×10^6
ΔA1	-20.98	11.71	-32.69	(5.36±1.03)×10^5
ΛB4	-22.94	16.58	-39.52	(8.41±1.55)×10^6
ΔB4	-23.08	13.89	-36.97	(3.01±0.29)×10^6

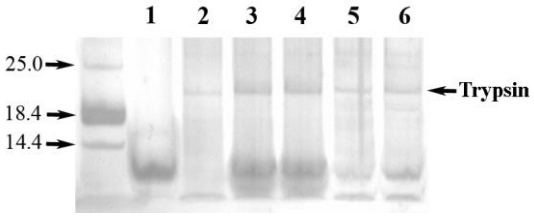

fig. S10. SDS-PAGE analysis of the effect of metallohelices on tryptic digests of Aβ12–28. 1) Aβ12-28 alone, **2**) Aβ12-28 digested by trypsin, **3**) ΔB4–Aβ12-28 digested by trypsin, **4**) ΛB4–Aβ12-28 digested by trypsin, **5**) ΔA1–Aβ12-28 digested by trypsin, **6**) ΛA1–Aβ12-28 digested by trypsin.

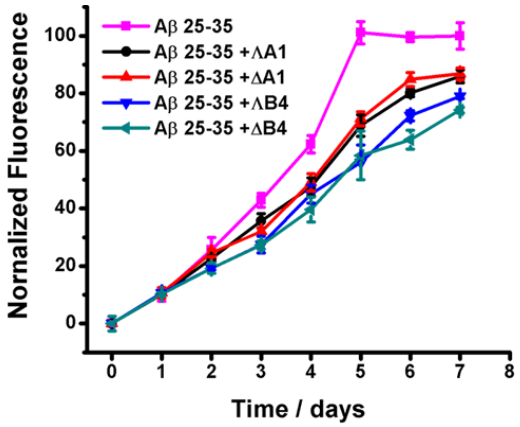

fig. S11. The aggregation kinetics of Aβ25–35 was monitored by the fluorescence of ThT in the absence or presence of A1 and B4. The concentration of Aβ25-35 was 50 μM, and the concentrations of metallohelices were 10 μM. Values exhibit mean ± SD and independent experiments were performed three times.

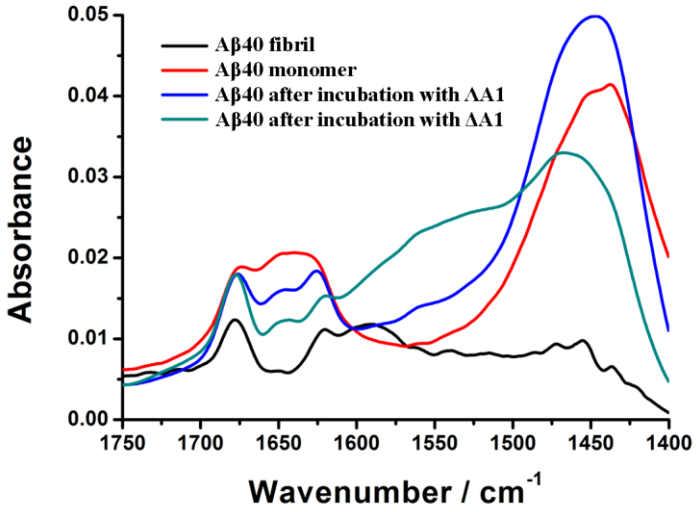

fig. S12. FTIR spectra of Aβ40 in different conditions. (For samples of Aβ40 fibril and monomer in water media, spectra of water are subtracted. For samples of Aβ40 with ΛA1 and ΔA1 treatment, spectra of metallohelices in water are subtracted.)

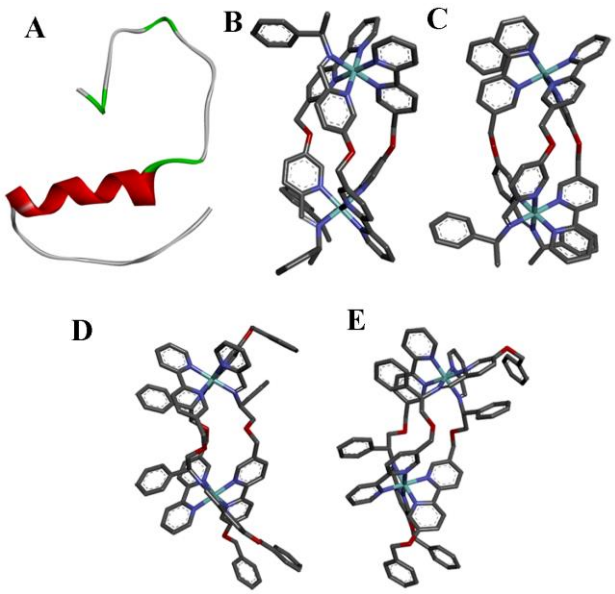

fig. S13. Structures of Aβ40 and metallohelices used for docking study. Structures of (**A**) Aβ40, (**B**) ΛA1, (**C**) ΔA1, (**D**) ΛB4 and (**E**) ΔB4 used for docking study.

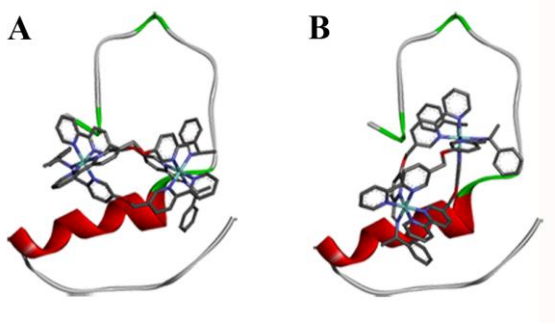

fig. S14. Energy-minimized average models of A1 with Aβ40 interactions.

Energy-minimized average models of (**A**) ΛA1, and (**B**) ΔA1 with Aβ40 interactions.

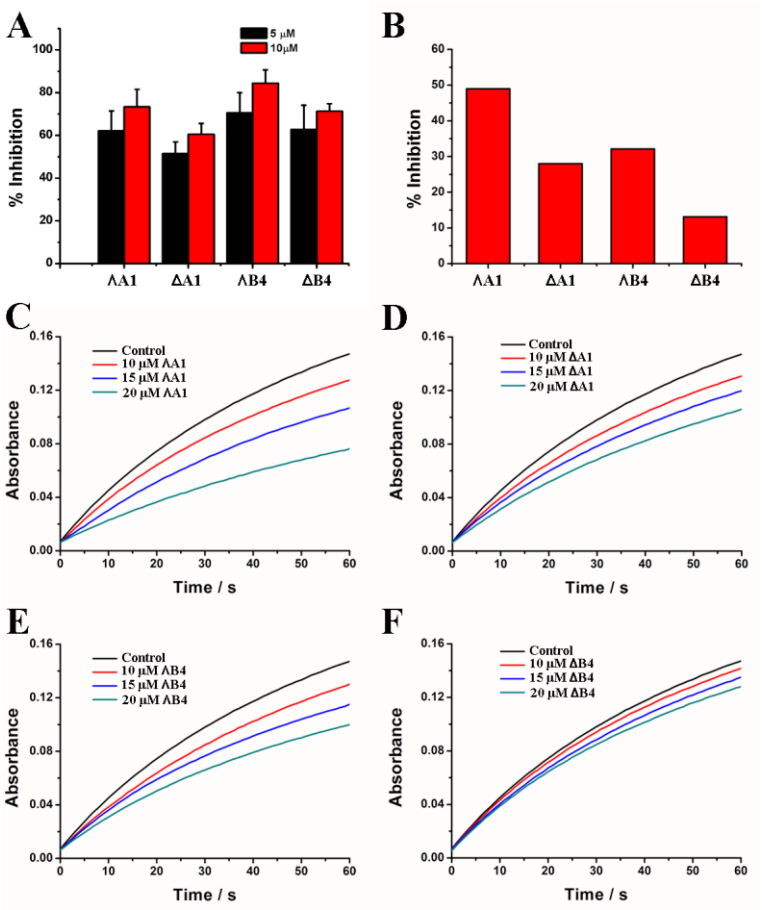

fig. S15. A1 and B4 scavenging ROS monitored by NBT and ABTS methods. (**A**) Percent inhibition of NBT oxidation by superoxide radicals generated in the riboflavin−NBT−light system in vitro assessed by NBT^+ absorption at 560 nm with metallohelices A1 and B4. Values exhibit mean ± SD and independent experiments were performed three times. (**B**) Percent inhibition of ABTS oxidation by metallohelices A1 and B4. (**C**-**D**) Oxidation of ABTS was inhibited by metallohelices ΛA1, ΔA1, ΛB4, and ΔB4 at difference concentration.

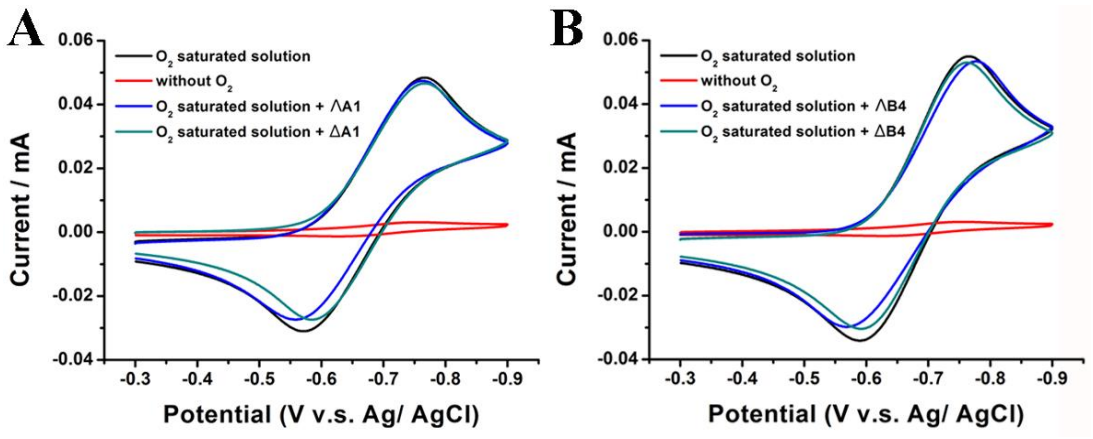

fig. S16. Cyclic voltammograms corresponding to the $O_2/O_2^{\bullet}$ redox couple. (**A**) The reactivity of ΛA1 and ΔA1 with superoxide. (**B**) The reactivity of ΛB4 and ΔB4 with superoxide. Sweep rate: 0.1 Vs^{-1}. Electrolytic media: DMSO + 0.1M TBAHFP (tetrabutylammonium hexafluoro phosphate).

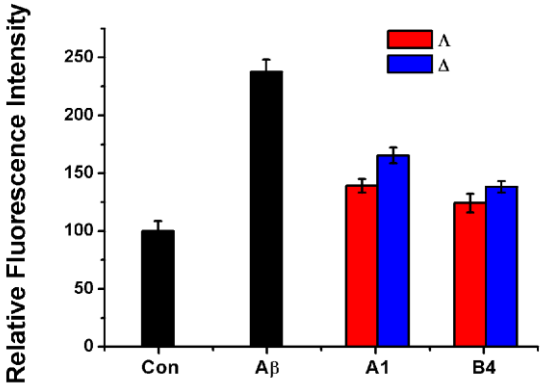

fig. S17. Effect of the metallohelices on ROS production in PC12 cells. Cells were treated with aged Aβ40 at a concentration of 5 μM in the absence or presence of increasing concentration of metallohelices, and 12 h later ROS generation inside the cells was measured using dichlorodihydrofluorescein (DCF) fluorescence. Values exhibit mean ± SD and independent experiments were performed three times.

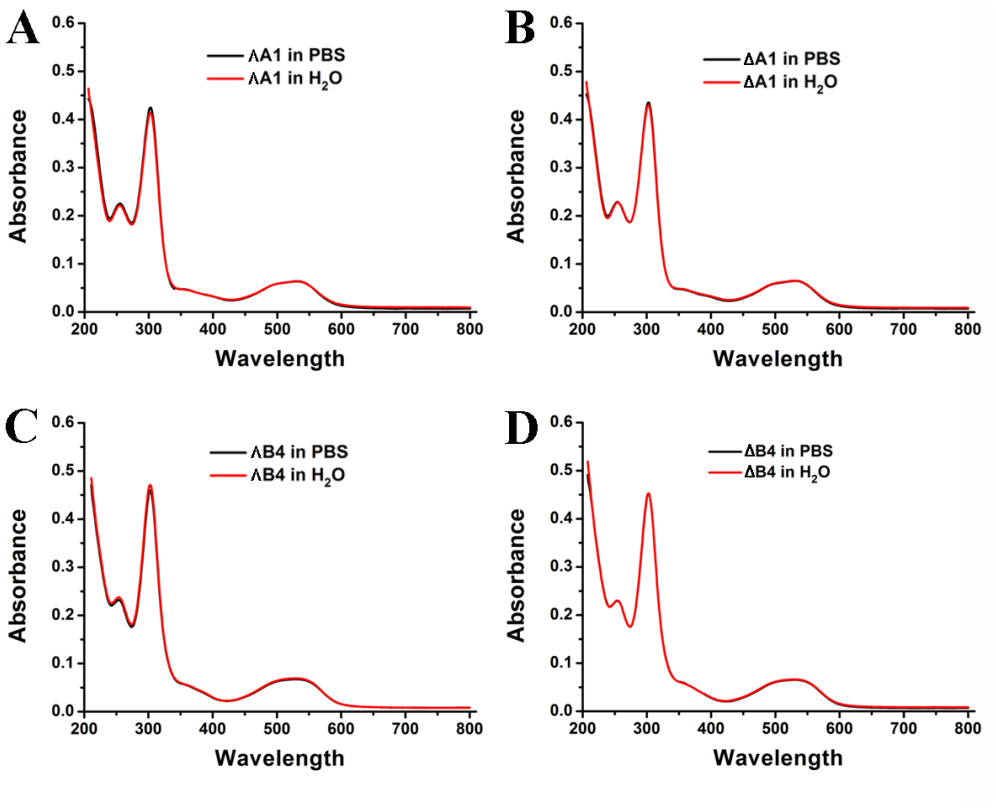

fig. S18. Absorption spectra of 5 μM metallohelices in water and PBS. (**A**) ΛA1, (**B**) ΔA1, (**C**) ΛB4, (**D**) ΔB4.

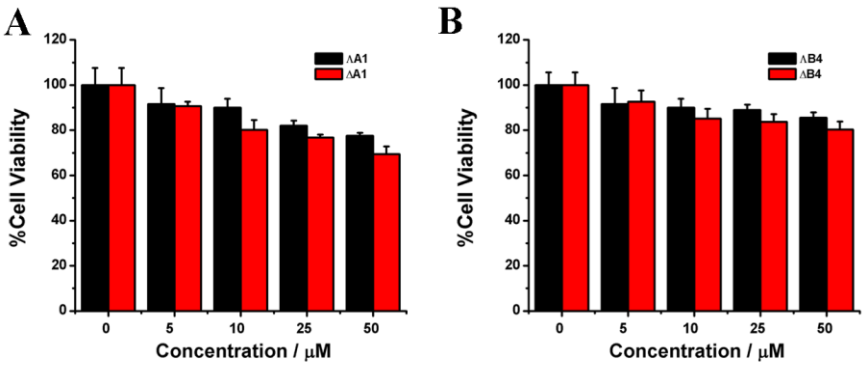

fig. S19. Effect of A1 and B4 on PC12 cell viability determined by MTT. Effect of (**A**) metallohelices A1 and (**B**) B4 on PC12 cell viability determined by MTT method. Values exhibit mean ± SD and independent experiments were performed three times.

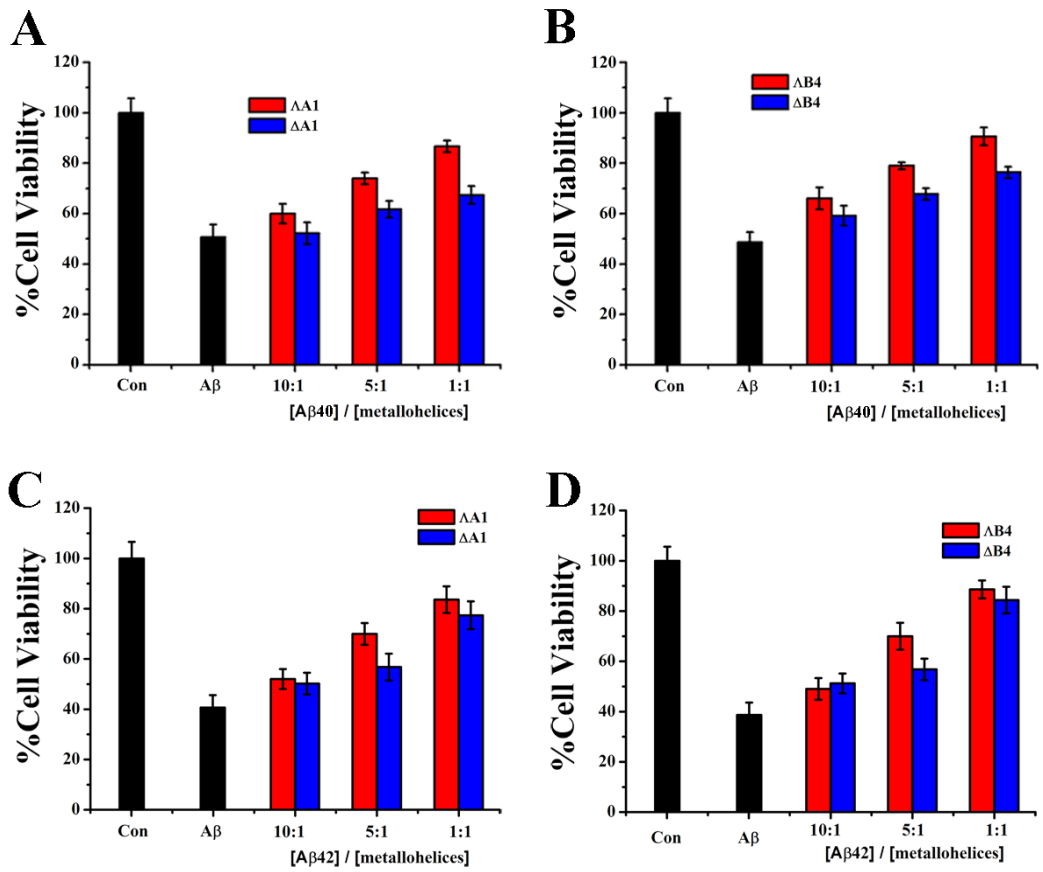

fig. S20. Protection effects of metallohelices on Aβ40- and Aβ42-induced cytotoxicity of PC12 cells. The concentration of Aβ40 was 5 μM. Values exhibit mean ± SD and independent experiments were performed three times.